Generalized Conditions for Hydraulic Criticality of Oceanic Overflows

LARRY PRATT AND KARL HELFRICH

Woods Hole Oceanographic Institution, Woods Hole, Massachusetts

(Manuscript received 11 November 2004, in final form 28 March 2005)

ABSTRACT

Two methods for assessing the hydraulic criticality of an observed or modeled overflow are discussed. The methods are valid for single-layer deep flows with arbitrary potential vorticity and cross section. The first method is based on a purely steady view in which the flow at a given section is divided up into a group of "streamtubes." A hydraulic analysis requires an extension of Gill's functional formulation to systems with many degrees of freedom. The general form of the critical condition and associated compatibility condition for such a system are derived and applied to the streamtube model. As an aside, it is shown by example that Gill's original critical condition can fail to capture all possible critical states, but that this problem is fixed when the multivariable approach is used. It is also shown how Gill's method can be applied to certain dispersive or dissipative systems. The second method of assessing criticality involves direct calculation of linear, long-wave speeds using a time-dependent version of the streamtube model. This approach turns out to be better suited to the analysis of geophysical datasets. The significance of the local Froude number F is discussed. It is argued that F must take on the value unity at some point across a critical section.

1. Introduction

Hydraulic criticality and control are concepts that date back to work by Reynolds (1886) and Hugoniot (1886) in the area of gas dynamics. The same ideas hold for steady, shallow flow over a dam and have more recently been applied to deep ocean overflows. In these applications, "critical flow" refers to a steady state that supports stationary nondispersive waves of small amplitude. In most cases the nondispersive waves are "long" waves, but there are exceptions (e.g., Baines and Leonard 1989). Changes in topography at a section of hydraulically critical flow lead to changes in the overflow transport and other properties. "Critical sections" often occur at points of constriction such as the crest of a dam or the narrowest section of a wind tunnel. It is also normal for the flow upstream of the constriction to be "subcritical," meaning that long-wave propagation in both up- and downstream directions is permitted, and for the downstream flow to be supercritical, meaning that propagation only in the downstream direction is permitted. The transition between subcritical and supercritical states occurs at or near the most constricted section and the flow there is said to be critical. Generalizations have been made to situations where the flow is bidirectional and "upstream" and "downstream" are less clearly defined (e.g., Armi 1986).

Hydraulic transitions and the occurrence of critical flow have profound implications for the physics of the flow. A hydraulic transition implies a downstream region of supercritical flow subject to enhanced mixing and entrainment and the formation of hydraulic jumps. Upstream effects are also important and include partial blocking of the transport and regulation of the stratification in the upstream basin. The critical condition can be used in principle to write down a "weir" formula relating the transport to hydrographic properties of the upstream flow (e.g., Whitehead 1989; Borenäs and Nikolopoulos 2000). Such formulas potentially serve as a basis for long-term monitoring of the transport (e.g., Hansen et al. 2001). Weir formulas traditionally assume that critical flow occurs at the sill, but nonconservative processes such as bottom drag and entrainment can cause the critical section to lie elsewhere (Pratt 1986; Gerdes et al. 2002) with consequences for the weir formula. All of these factors make the diagnosis of flow criticality and the location of the critical section important in the analysis of deep ocean overflows and of other hydraulically driven flows of geophysical relevance.

Corresponding author address: Larry Pratt, Mail Stop 21, 360 Woods Hole Rd., Woods Hole, MA 02543.
E-mail: lpratt@whoi.edu

© 2005 American Meteorological Society

For nonrotating, homogeneous, shallow, free-surface flows, the standard indicator of the hydraulic state at a given cross section is the Froude number $v/(gd)^{1/2}$, with v denoting the depth-independent horizontal velocity, d the fluid depth, and g the gravitational acceleration. This result can be generalized to a deep layer flowing underneath an inactive upper layer, and the appropriate Froude number is obtained by reducing g in proportion to the relative density difference between the two layers. The flow is subcritical, critical, or supercritical depending on whether $v/(gd)^{1/2}$ is <1, $=1$, or >1, an interpretation valid where the variation of v and d across the flow is weak. Although this assumption may be valid for certain streams and open channels there are other applications where such variations are large and where the appropriate Froude number is not known. Examples include the deep ocean overflows such as those of the Denmark Strait, the Faroe–Bank Channel, the Jungfern Passage, and the Vema Channel. The combination of rotation and complicated cross-sectional geometry lead to significant variations in v and d across the passage in question.

The belief that subcritical-to-supercritical transitions take place is founded on the observed "overflow" character itself: the spilling of dense water from one ocean basin into another. The upstream/downstream asymmetry and resemblance to flow over a dam has led to the presumption that hydraulic transitions are taking place, but this conjecture has almost never been verified by direct measurement in settings where rotation is strong. Theories for homogeneous, rotating-channel flow (i.e., Whitehead et al. 1974; Stern 1974; Gill 1977; Borenäs and Lundberg 1986) have resulted in the formulation of generalized Froude numbers, but application is often limited by inherent idealizations such as restriction to a rectangular cross section or to uniform potential vorticity. Here we will present two new measures of criticality that are less restricted. Both are based on a multiple streamtube representation of an overflow, constructed by dividing observed flow at a particular section into transport and energy conserving subsections. The first measure is obtained by asking whether a stationary wave can exist at the section in question. Development of the formal criterion requires that one generalize the Gill (1977) approach (reviewed in section 2) to a system with an arbitrary number of degrees of freedom (section 3). The general form of the critical condition and associated compatibility condition for such a system are derived and applied to the streamtube model (section 4). As an aside, it is shown by example that Gill's original critical condition can fail to capture all possible critical states, but that this problem is fixed when the multivariable approach is used. As it turns out, the criterion is well suited in application to an analytically or numerically modeled flow, but requires more data than are typically available in field studies. A second condition based on direct calculation of long-wave speeds is then developed (section 5) and shown to be better suited to oceanic data. The wave speed calculation is based on a time-dependent version of the multiple streamtube model and the result is directly tied in to the extended Gill formulation for steady flow.

This work also addresses several issues closely connected to the concept of hydraulic criticality. One concerns the significance of the local Froude number F in cases where this quantity varies across the flow (section 6). We discuss the differences between local propagation of free disturbances and hydraulic control with respect to a normal mode. A result of this discussion will be the conjecture that F must equal unity at some point across the section in order for the flow to be hydraulically critical with respect to a long normal mode. We also discuss the conditions for hydraulically criticality in certain cases in which traditional hydraulic approximations are invalid (appendix A).

2. Hydraulics in a single variable: The Gill (1977) approach

If "hydraulic criticality" is defined as a steady flow state that supports stationary long waves of infinitesimal amplitude, then the methodology of Gill (1977) can be used to write down conditions for critical flow. The approach applies to a steady, conservative flow in a conduit or waveguide that varies gradually in the longitudinal (y) direction. Conserved properties might include volume and/or mass flux, energy, density (or potential density), and vorticity (or potential vorticity). It was assumed by Gill that the corresponding conservation laws can be combined, reducing the number of dependent variables to a single unknown $\gamma(y)$. For flow in a rotating channel of rectangular cross section $\gamma(y)$ is often chosen as the average of the layer thicknesses on the two side walls. Knowledge of $\gamma(y)$ at a particular "section" y of the conduit determines all the flow characteristics (depth, pressure, etc.) at that section. The conservation laws relate $\gamma(y)$ to the local geometric properties of the conduit $h(y)$, $w(y)$, and so on by an equation of the form

$$G[\gamma(y); h(y), w(y), \ldots; B, Q, \ldots] = C, \qquad (2.1)$$

where C is a constant. For example, $h(y)$ and $w(y)$ could represent the bottom elevation and width of a channel of rectangular cross section. The relation (2.1) also depends on parameters B, Q, and so on, corresponding to the values of the conserved quantities. By

definition

$$\frac{dG}{dy} = \frac{\partial G}{\partial \gamma}\frac{d\gamma}{dy} + \frac{\partial G}{\partial h}\frac{dh}{dy} + \frac{\partial G}{\partial w}\frac{dw}{dy} + \cdots = 0, \qquad (2.2)$$

which is often just the differential form of a momentum or continuity equation.

Now consider the conditions under which free, stationary long waves of small amplitude exist. By "long waves" we mean disturbances that vary gradually in the y direction, just as the steady flow does. By "free" we mean disturbances that occur spontaneously and are independent of any forcing mechanism, including bottom slope. When a steady flow becomes hydraulically critical at a particular section $y = y_c$, it can support a stationary disturbance at that section. In other words, the steady state can be locally altered without changing either the conduit geometry or the upstream conditions. The altered flow must therefore have the same volume flux, energy, and so on, as the undisturbed flow and G must have the same value. In formal terms, there must exist a small disturbance that preserves the value of G and is free of variations in h, w, and so on:

$$(\delta G)_{w,h,\ldots} = \frac{\partial G}{\partial \gamma}\, d\gamma = 0 \quad \text{or} \quad \frac{\partial G}{\partial \gamma} = 0. \qquad (2.3)$$

Here and elsewhere the notation $(\,)_{x,y,\ldots}$ means that x, y, . . . are held constant while the operation in parentheses is carried out.

As an example, consider a nonrotating, two-dimensional, free-surface flow passing over a bottom of variable elevation h (Fig. 1). If the flow at the sill is hydraulically critical, a localized, infinitesimal disturbance of the fluid depth d and velocity v may exist there. The amplitude and shape of the disturbance may be regarded as arbitrary as long as it is recognized that the disturbance is small. The disturbed flow (dashed line) has the same upstream state and therefore the same volume flow rate per unit width $Q = vd$ and energy per unit mass (Bernoulli function) $B = (v^2/2) + gd + gh$ as the original. Substituting for v in the expression of the Bernoulli function leads to a conservation law in the single variable d:

$$G(d; h) = \frac{Q^2}{2d^2} + gd + gh = B \qquad (2.4)$$

with B and Q constant. Applying (2.3) with d now playing the role of γ yields the well-known critical condition $Q = g^{1/2}d^{3/2}$, or $v = (gd)^{1/2}$.

The flow at a critical section is particularly vulnerable to external forcing. In the case of the 1D flow governed by (2.4) the stationary wave is a long (and therefore nondispersive) gravity wave. At a critical section, the long wave will be resonantly excited by stationary forcing. Since the group velocity of the stationary wave is zero, disturbance energy is unable to escape and will increase with time, presumably leading to a dramatic change in the background flow. This behavior distinguishes stationary long waves from lee waves, which are stationary waves of finite length. The latter are dispersive and allow energy to propagate away even though the phase speed is zero.

The threat of long-wave resonance suggests that critical flow can only occur where the topography does not force the flow. This idea can be put on formal ground by evaluating (2.2) at a critical section $(\partial G/\partial \gamma)_{y=y_c} = 0$ and assuming that the flow remains smooth as it passes through the critical section ($d\gamma/dy$ exists and is bounded at y_c). It follows that

$$\left(\frac{\partial G}{\partial h}\frac{dh}{dy} + \frac{\partial G}{\partial w}\frac{dw}{dy} + \cdots\right)_{y=y_c} = 0. \qquad (2.5)$$

This "regularity" condition restricts the locations $y = y_c$ at which critical flow can occur and allow smooth computation of solutions through those locations. These locations are sometimes called *control* sections. Applying (2.5) to (2.4) leads to the conclusion that critical flow can occur only where $dh/dy = 0$, as at a sill.

Their nondispersive nature is just one of the properties that makes long waves (as opposed to other stationary disturbances) centrally important in hydraulics. Another is that long waves project exactly on the steady flows that they modify. In the case of the shallow flow governed by (2.4) both the steady flow and the long waves have depth-independent horizontal velocity, whereas surface gravity waves of finite length have depth-decaying horizontal velocity. A second reason is that the long-wave resonance described above makes steady flow particularly vulnerable to changes the conduit constriction. Imagine a steady flow over a dam and consider the consequences of raising the crest of the dam slightly. If the depth and velocity of the crest flow is initially d_0 and v_0, then $v_0 - (gd_0)^{1/2}$ is initially zero at the crest. The change in crest elevation excites a stationary long waves and its energy builds until the disturbance acquires finite amplitude. Its speed can now exceed the linear value $v_0 - (gd_0)^{1/2}$ and it can break free and propagate upstream, altering the upstream flow. Numerous demonstrations of this and similar processes can be found in the literature, beginning with Long's (1954) towing experiments and including many numerical extensions Baines (1995) and Pratt et al. (2000).

In most applications, critical flow occurs at a section (or sections) $y = y_c$ marking the transition between states supporting wave propagation in different direc-

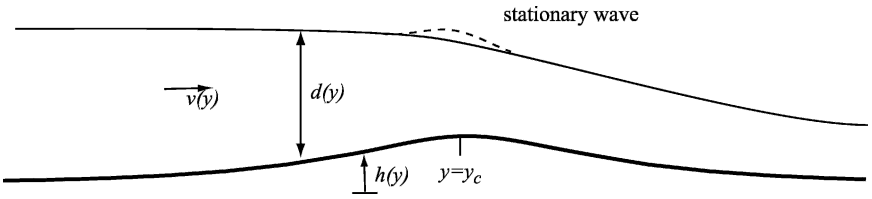

FIG. 1. Definition sketch for shallow, homogeneous flow over topography.

tions. Strictly speaking, the flow is able to support stationary disturbances only at y_c and not at points immediately upstream and downstream as suggested in Fig. 1. The stationary disturbances are therefore possible in theory but are difficult to visualize in most applications. They should not be confused with stationary lee waves, which involve waves of finite length.

The form (2.1) of the functional G used by Gill is based on the presumption that the flow state at a given y depends only on the characteristics of the conduit at that y (and on the values of the parameters Q, B, etc.). Nonlocal dependence on y can occur in systems that exhibit hydraulic behavior, either as a result of dissipation or of variations in geometry that are nongradual. In appendix A, we give two examples of such systems and show how the Gill approach can be extended and used to find a critical condition. One involves a system in which the short, rather than long, waves are nondispersive.

3. Extending the Gill approach to systems with multiple variables

Reduction of the problem to the single-variable format envisioned by Gill (1977) is not always easy. It is often more convenient, and sometimes necessary, to work with two independent relations in two variables γ_1 and γ_2:

$$G_1(\gamma_1, \gamma_2; h, w, \ldots; B, Q, \ldots) = C_1 \tag{3.1}$$

and

$$G_2(\gamma_1, \gamma_2; h, w, \ldots; B, Q, \ldots) = C_2. \tag{3.2}$$

The existence of a stationary wave now requires that small variations $d\gamma_1$ and $d\gamma_2$ can be found such that G_1 and G_2 both remain fixed. Thus

$$(\delta G_1)_{w,h,\ldots} = \frac{\partial G_1}{\partial \gamma_1} d\gamma_1 + \frac{\partial G_1}{\partial \gamma_2} d\gamma_2 = 0 \tag{3.3}$$

and

$$(\delta G_2)_{w,h,\ldots} = \frac{\partial G_2}{\partial \gamma_1} d\gamma_1 + \frac{\partial G_2}{\partial \gamma_2} d\gamma_2 = 0. \tag{3.4}$$

The critical condition is just the solvability condition for (3.3) and (3.4):

$$\frac{\partial G_1}{\partial \gamma_1}\frac{\partial G_2}{\partial \gamma_2} - \frac{\partial G_1}{\partial \gamma_2}\frac{\partial G_2}{\partial \gamma_1} = 0, \tag{3.5}$$

first obtained by Pratt and Armi (1987). Stationary waves then involve the tangent displacement $(d\gamma_1, d\gamma_2)$ as given by (3.3) or (3.4):

$$d\boldsymbol{\gamma} = d\gamma_1 \left[1, -\left(\frac{\partial G_1/\partial \gamma_1}{\partial G_1/\partial \gamma_2}\right)_{y_c}\right], \tag{3.6}$$

where $d\gamma_1$ is small but arbitrary. The displacement vector contains information about the cross-sectional structure of the stationary wave.

The generalization of the regularity condition (2.5) can be found by writing out the identities $dG_1/dy = 0$ and $dG_2/dy = 0$:

$$\frac{dG_1}{dy} = \frac{\partial G_1}{\partial \gamma_1}\frac{d\gamma_1}{dy} + \frac{\partial G_1}{\partial \gamma_2}\frac{d\gamma_2}{dy} + \frac{\partial G_1}{\partial h}\frac{dh}{dy} + \frac{\partial G_1}{\partial w}\frac{dw}{dy} + \cdots = 0 \tag{3.7a}$$

and

$$\frac{dG_2}{dy} = \frac{\partial G_2}{\partial \gamma_1}\frac{d\gamma_1}{dy} + \frac{\partial G_2}{\partial \gamma_2}\frac{d\gamma_2}{dy} + \frac{\partial G_2}{\partial h}\frac{dh}{dy} + \frac{\partial G_2}{\partial w}\frac{dw}{dy} + \cdots = 0. \tag{3.7b}$$

Solving for $d\gamma_1/dy$ leads to

$$\frac{d\gamma_1}{dy} = \frac{\dfrac{\partial G_1}{\partial \gamma_2}\left(\dfrac{\partial G_2}{\partial y}\right)_{\gamma_1,\gamma_2} - \dfrac{\partial G_2}{\partial \gamma_2}\left(\dfrac{\partial G_1}{\partial y}\right)_{\gamma_1,\gamma_2}}{\dfrac{\partial G_1}{\partial \gamma_1}\dfrac{\partial G_2}{\partial \gamma_2} - \dfrac{\partial G_1}{\partial \gamma_2}\dfrac{\partial G_2}{\partial \gamma_1}}, \tag{3.8}$$

where $[\partial(\,)/\partial y]_{\gamma_1,\gamma_2} = [\partial(\,)/\partial w](\partial w/\partial y) + [\partial(\,)/\partial h](\partial h/\partial y) + \cdots$ is a derivative taken with γ_1 and γ_2 held constant. Critical flow requires that the denominator vanish and the numerator must then vanish if the flow is to remain well behaved. The regularity condition is thus

$$\left.\frac{\partial G_1}{\partial \gamma_i}\frac{\partial G_2}{\partial y}\right|_{\gamma_1,\gamma_2} - \left.\frac{\partial G_2}{\partial \gamma_i}\frac{\partial G_1}{\partial y}\right|_{\gamma_1,\gamma_2} = 0 \ (i = 1 \text{ or } i = 2), \tag{3.9}$$

(The $i = 2$ version, which follows from developing an expression for $d\gamma_2/dy$, is not independent of the $i = 1$ version.)

Dalziel (1991) showed that two-layer hydraulics with no rotation can be formulated using two functionals of

the forms (3.1) and (3.2). He derives the well-known critical condition (e.g., Armi 1986) equivalent to setting a composite Froude number to unity (e.g., Armi 1986); however, (3.5), (3.6), or (3.9) are never explicitly written down. The stationary disturbance in this case is an internal wave and the relationship (3.6) linking $d\gamma_1$ and $d\gamma_2$ determines the ratio of the amplitudes of the wave in the two layers.[1] In Smeed's (2000) treatment of three-layer exchange flow, the hydraulics problem is again reduced to two functional relations of the required form and (3.5) and (3.9) are derived.

The machinery can be extended to problems governed by N relations for N independent variables:

$$\begin{aligned}
&G_1[\gamma_1(y), \gamma_2(y), \gamma_3(y), \ldots, \gamma_N(y);\\
&\qquad h(y), w(y), \ldots, B, Q, \ldots] = C_1\\
&G_2[\gamma_1(y), \gamma_2(y), \gamma_3(y), \ldots, \gamma_N(y);\\
&\qquad h(y), w(y), \ldots, B, Q, \ldots] = C_2\\
&\qquad\qquad \vdots\\
&G_N[\gamma_1(y), \gamma_2(y), \gamma_3(y), \ldots, \gamma_N(y);\\
&\qquad h(y), w(y), \ldots, B, Q, \ldots] = C_N. \qquad (3.10)
\end{aligned}$$

The condition for stationary waves is now

$$(\delta G_i)_{h,w,\ldots} = \sum_{j=1}^{N} \frac{\partial G_i}{\partial \gamma_j} d\gamma_j = 0 \ (i = 1, 2, \ldots, N), \qquad (3.11)$$

and the corresponding solvability condition is the vanishing of a generalized Jacobian:

$$\det\left(\frac{\partial G_i}{\partial \gamma_j}\right) = 0, \qquad (3.12)$$

where

$$\left(\frac{\partial G_i}{\partial \gamma_j}\right) = \begin{pmatrix} \partial G_1/\partial\gamma_1 & \cdots & \partial G_1/\partial\gamma_N \\ \vdots & \ddots & \vdots \\ \partial G_N/\partial\gamma_1 & \cdots & \partial G_N/\partial\gamma_N \end{pmatrix}. \qquad (3.13)$$

The tangent displacement vector $(d\gamma_1, d\gamma_2, \ldots)_c$, which is computed from any member of (3.11), again determines the transverse structure of the stationary wave.

A generalized regularity condition for critical flow can also be obtained. Since $dG_i/dy = 0$ it follows from (3.12) that

$$\frac{\partial G_i}{\partial \gamma_1}\frac{d\gamma_1}{dy} + \frac{\partial G_i}{\partial \gamma_2}\frac{d\gamma_2}{dy} + \cdots + \frac{\partial G_i}{\partial \gamma_N}\frac{d\gamma_N}{dy} = -\left(\frac{\partial G_i}{\partial y}\right)_\gamma, \qquad (3.14)$$

where $(\partial/\partial y)_\gamma$ denotes a derivative with γ_1, γ_2, and so on, held fixed. From Cramer's rule, it follows that

$$\frac{d\gamma_i}{dy} = -\frac{\det\left[\left(\dfrac{\partial G_i}{\partial \gamma_j}\right)^{\mathrm{T}} \middle| \left(\dfrac{\partial G_i}{\partial y}\right)_\gamma^{\mathrm{T}}\right]}{\det\left(\dfrac{\partial G_i}{\partial \gamma_j}\right)^{\mathrm{T}}}, \qquad (3.15)$$

where $(\partial G_i/\partial\gamma_j)|(\partial G_i/\partial y)_\gamma$ is the matrix obtained by replacing the ith column of $(\partial G_i/\partial\gamma_j)$ by

$$\left(\frac{\partial G_i}{\partial y}\right)_\gamma = \begin{bmatrix} (\partial G_1/\partial y)_\gamma \\ (\partial G_2/\partial y)_\gamma \\ \vdots \\ (\partial G_N/\partial y)_\gamma \end{bmatrix}.$$

Critical flow occurs when the denominator of the right-hand side of (3.15) vanishes. To insure that the derivatives on the left-hand side remain bounded, the numerator must also vanish:

$$\det\left[\left(\frac{\partial G_i}{\partial \gamma_j}\right)^{\mathrm{T}} \middle| \left(\frac{\partial G_i}{\partial y}\right)_\gamma^{\mathrm{T}}\right] = 0. \qquad (3.16)$$

This is the regularity condition.

When hydraulic models are formulated directly from the differential form of the equations of motion, as is sometimes done with two-dimensional, multilayer flow, a constraint of the form (3.15) is obtained directly (e.g., Engqvist 1996). The critical condition is then identified as the vanishing of the denominator of the right-hand side, implying (3.16). This provides a link with the Gill formulation. One must be prepared to explain why the vanishing of the denominator implies critical flow; here an insightful person might cite the resonance condition described earlier.

In some cases, there may be an advantage to working with a number of dependent variables, even though that number can be reduced to one by algebra. As an example, consider the hydraulics of a rotating layer of zero potential vorticity flowing along a wall and over a horizontal bottom of elevation h (Fig. 2). As shown by Stern (1980) the flow state at any section can be described by its width w_e and the value of the alongshore velocity v_e at its free, offshore edge. The alongshore evolution of these quantities can be calculated from conservation of volume flux:

$$\frac{1}{2} w_e^2 \left(v_e - \frac{1}{2} w_e\right)^2 = Q \qquad (3.17)$$

[1] When d_1 and d_2 are used as dependent variables, the relationship (3.6) between the displacements in the two layers is made trivial by the geometric constraint (3.8). However, if the layer velocities were used as dependent variables, (3.6) would yield a nontrivial relation between the velocity perturbations in each layer because of the stationary internal wave.

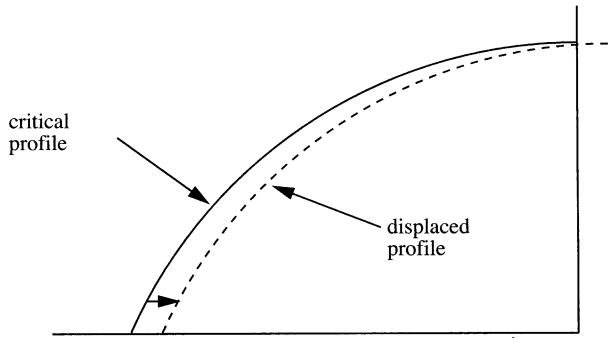

FIG. 2. A zero-potential-vorticity coastal current with width w_e and alongshore velocity v_e at the free edge. The current is hydraulically critical when the slope of the interface (and therefore the alongshore velocity) is zero at the wall. The stationary wave is manifested by an infinitesimal uniform displacement of the entire current, onshore or offshore, as suggested by the dashed line. The value of v_e is unaffected by this displacement.

and energy

$$\frac{v_e^2}{2} + h = B \tag{3.18}$$

(both in nondimensional form). It can also be shown by direct calculation of the long-wave speeds for this system that the flow is hydraulically critical when $w_e = v_e$ or when $v_e = 0$. (However, the latter corresponds to a limiting case where the water depth and velocity go to zero all across the flow.)

An unusual feature of (3.18) is that it appears to satisfy all the requirements for a Gill functional (2.1) in a single the variable (v_e). It would appear that one could solve the hydraulic problem using (3.18) alone. However, if one defines $G(v_e; h) = (\frac{1}{2})v_e^2 + h$ and applies the Gill critical condition $\partial G/\partial v_e = 0$, the solution $v_e = 0$ misses the most pertinent condition, $w_e = v_e$. If instead (3.17) and (3.18) are treated as a two-by-two system and (3.5) is applied, both critical conditions follow. The physical explanation behind the apparent failure of Gill's original approach is that the stationary wave in question is manifested by an offshore excursion dw_e in the position of the free edge (Fig. 2) with no corresponding variation in the free edge velocity, (i.e., $dv_e = 0$). A search for this stationary wave using the requirement $\partial G/\partial v_e = 0$ comes up empty.

As discussed in appendix B, the above formalism can be adapted to a continuous system. The index j is replaced by a continuous variable such as the streamfunction ψ. A functional expressing conservation of a property such as energy exists for each ψ. We show that the critical condition for such a system is that a nontrivial solution to a particular homogeneous equation exists. The equations contain coefficients that depend on the flow state, that these coefficients must be specialized in order for a nontrivial solution to exist. The result is analogous to the solvability condition for (3.7) and examples pertaining to continuously stratified, nonrotating, and rotating flow have been documented by Killworth (1992, 1995). Unless the homogeneous equation is quite simple, however, there is no established analytical procedure for specializing the coefficients. Progress then requires one to consider a discrete approximation to the continuous system and to find a solvability condition for the resulting finite set of equations, an exercise tantamount to solving (3.12).

4. Assessing hydraulic criticality using a steady, multiple streamtube model

Consider a steady, reduced-gravity flow at a particular cross section of a deep, rotating strait (Fig. 3a). The elevation of the interface is denoted $\eta(x)$, where x is the cross-stream coordinate, and the along-strait velocity v is geostrophically balanced:

$$fv = g'\frac{\partial \eta}{\partial x}. \tag{4.1}$$

Density stratification is the most commonly measured physical property of such flows and we will assume that several such measurements have been taken at discrete positions $x_1, x_2, \ldots$ across the section in question (Fig. 3b). By identifying the density interface at each position the values $\eta(x_n)$ are found. We will also assume that the topographic height $h(x)$ and the positions $x = x_1$ and $x = x_{N+1}$ of the left and right edges of the lower layer are known. Then it is convenient to divide the observed flow into N segments (Fig. 3b), with the nth element extending from x_n to x_{n+1}.

We wish to examine the possibility that free, stationary, long disturbances can exist in the observed flow. In so doing, we will think of the sides of each element as streamlines and the elements themselves as streamtubes. The introduction of a stationary disturbance alters the positions of the streamlines but not the volume flux nor energy within each tube. In other words, the sides of the elements may move laterally and the corresponding values of η_n may change but the volume flux Q_n and energy B_n across each element remain fixed. The statements of volume flux conservation may be approximated as

$$\begin{aligned} Q_n &= \bar{v}_n \frac{d_n + d_{n+1}}{2}(x_{n+1} - x_n) \\ &= \frac{g'}{2f}(\eta_{n+1} - \eta_n)[\eta_{n+1} + \eta_n - h(x_{n+1}) - h(x_n)], \end{aligned} \tag{4.2}$$

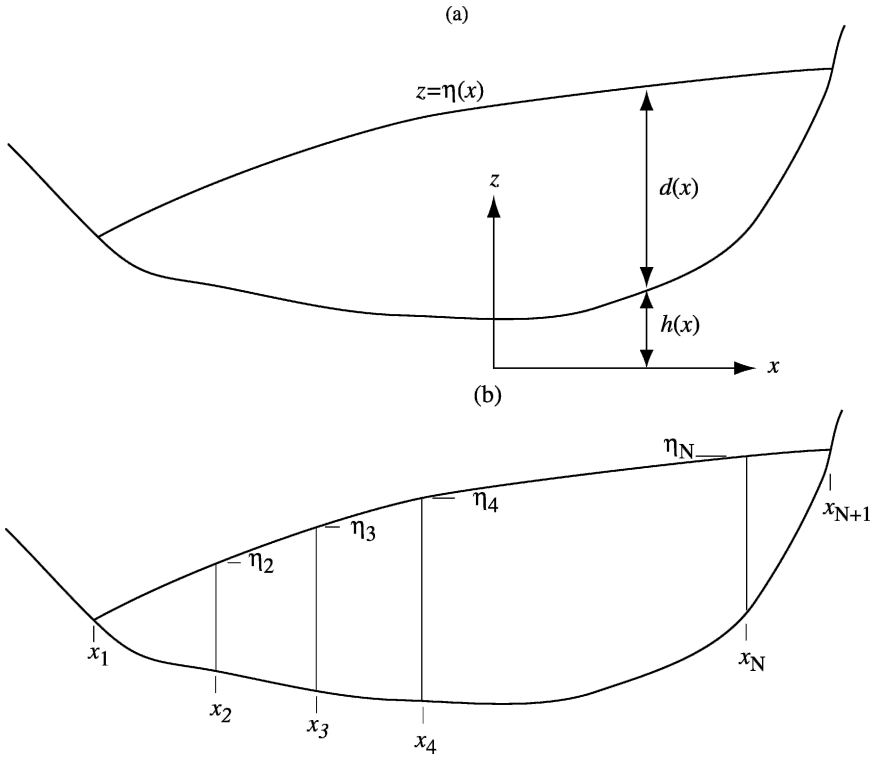

FIG. 3. (a) Definition sketch showing channel bottom and interface bounding a deep, homogeneous layer flowing underneath an inactive upper layer. The along-channel (y) velocity is in geostrophic balance. (b) Subdivision of the deep current into streamtube elements.

where the average velocity $\bar{v}$ for a given element has been related to the interface elevation using (4.1). Conservation of energy takes the approximate form

$$B_n \cong \frac{\bar{v}_n^2}{2} + g'\bar{\eta}_n \cong \frac{g'^2}{2f^2}\frac{(\eta_{n+1} - \eta_n)^2}{(x_{n+1} - x_n)^2} + \frac{g'}{2}(\eta_{n+1} + \eta_n). \tag{4.3}$$

Equations (4.2) and (4.3) form a system of $2N$ equations in terms of $2N$ variables. The latter are composed of the $N + 1$ streamline positions x_n and the $N - 1$ values of $\eta_2, \eta_3, \ldots, \eta_N$. [Note that the grounding of the flow at either edge means that the corresponding elevations $\eta_1 = h(x_1)$ and $\eta_{N+1} = h(x_{N+1})$ are not independent of x_1 and x_{N+1}.] Applying (3.12) therefore leads to the critical condition:

$$\det[\mathbf{b}] = 0, \tag{4.4}$$

where

$$\mathbf{b} = \begin{pmatrix} \partial B_1/\partial x_1 & \partial B_1/\partial x_2 & \cdots & \partial B_1/\partial x_{N+1} & \partial B_1/\partial \eta_2 & \partial B_1/\partial \eta_3 & \cdots & \partial B_1/\partial \eta_N \\ \partial B_2/\partial x_1 & \partial B_2/\partial x_2 & \cdots & \partial B_2/\partial x_{N+1} & \partial B_2/\partial \eta_2 & \cdots & \cdots & \partial B_2/\partial \eta_N \\ \vdots & \vdots & \ddots & \vdots & \vdots & \cdots & \ddots & \vdots \\ \partial B_N/\partial x_1 & \partial B_N/\partial x_2 & \cdots & \partial B_N/\partial x_{N+1} & \partial B_N/\partial \eta_2 & \partial B_N/\partial \eta_3 & \cdots & \partial B_N/\partial \eta_N \\ \partial Q_1/\partial x_1 & \partial Q_1/\partial x_2 & \cdots & \partial Q_1/\partial x_{N+1} & \partial Q_1/\partial \eta_2 & \partial Q_1/\partial \eta_3 & \cdots & \partial Q_1/\partial \eta_N \\ \partial Q_2/\partial x_1 & \partial Q_2/\partial x_2 & \cdots & \partial Q_2/\partial x_{N+1} & \partial Q_2/\partial \eta_2 & \cdots & \cdots & \partial Q_2/\partial \eta_N \\ \vdots & \vdots & \ddots & \vdots & \vdots & \cdots & \ddots & \vdots \\ \partial Q_N/\partial x_1 & \partial Q_N/\partial x_2 & \cdots & \partial Q_N/\partial x_{N+1} & \partial Q_N/\partial \eta_2 & \partial Q_N/\partial \eta_3 & \cdots & \partial Q_N/\partial \eta_N \end{pmatrix}. \tag{4.5}$$

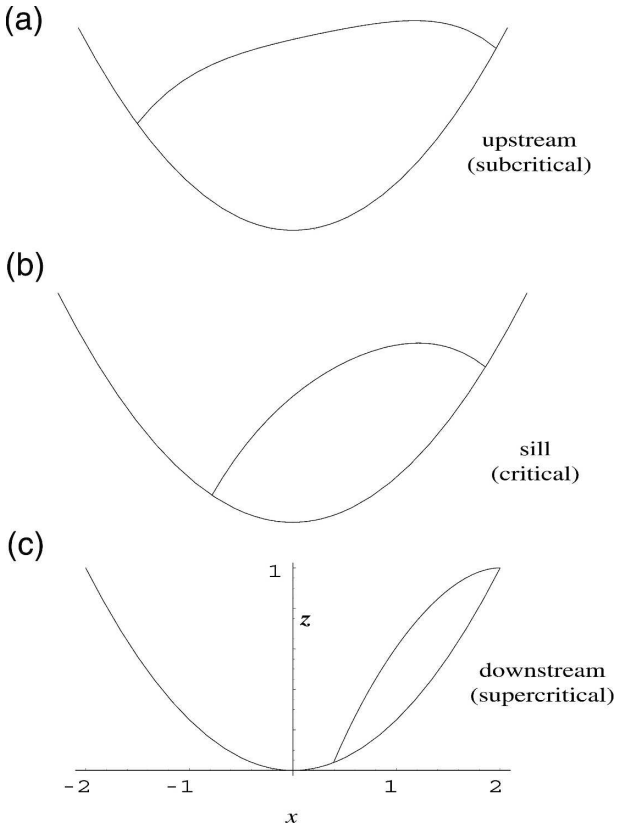

FIG. 4. Three cross sections showing flow with uniform potential vorticity in a parabolic channel [see (6.5)] with $\alpha = 0.25$. The solutions were calculated using the expressions appearing in Borenäs and Lundberg (1986) with dimensionless transport $Q = 1$ and with the upstream boundary layer portioning parameter set at $\psi_i/Q = 0.5$. The values of h_0 are (a) 0, (b) 0.25, and (c) 0. The flow is viewed from the upstream side.

We consider two applications, both to flow in rotating channels with parabolic cross sections:

$$h(x, y) = h_0(y) + \alpha x^2. \tag{4.6}$$

If the potential vorticity of the fluid is uniform then solutions along the whole length of channel can be found analytically from expressions developed by Borenäs and Lundberg (1986). It is also possible to write down a generalized Froude number giving the criticality of the flow at a given section. More details are given in appendix C. We have calculated several solutions for hydraulically controlled flow corresponding to different upstream conditions. The critical section occurs at a sill corresponding to a maximum in h_0. Cross sections of the flow for a case in which α is held fixed at 0.25 are shown in Fig. 4. Upstream of the sill (top panel) the flow is subcritical and relatively deep. The interface slopes up with positive x over most of the section, indicating positive velocity, although there is a narrow band of reverse flow on the right wall. At the sill the flow is critical, the overall layer thickness is smaller, and there is a more prominent band of reverse flow along the right wall. At the downstream section, the layer thickness is quite small, the velocity is positive all across the section, and the current is strongly banked against the right wall.

To evaluate the critical condition (4.4), the flow at each section is partitioned into three segments of equal width ($N = 3$), leading to a 6×6 matrix **b**. The value of det[**b**] is evaluated at a number of sections extending from upstream to downstream of the sill. In principle det[**b**] should change sign where the Froude number F_p [from (C.1)] crosses through unity, and Fig. 5a shows that this is very nearly the case. [The actual crossing is at $F \cong 0.93$.] Similar results hold for solutions calculated with $\alpha = 1$ and $\alpha = 4$, with the zero crossings at $F \cong 0.98$ and $F \cong 0.99$, respectively; $N = 3$ therefore appears to provide reasonably good resolution.

The magnitude of det[**b**] is quite small in the subcritical ($F < 1$) range relative to the supercritical range (Fig. 5a), also characteristic of the other cases analyzed. If the analysis had been based on field or laboratory data with accompanying noise, it is quite possible that the value of det[**b**] would be judged indistinguishable from zero at all upstream sections. This situation would cloud interpretation of the results. An alternative is to calculate the eigenvalues $\chi_1, \chi_2, \chi_3, \ldots, \chi_{2N}$ of **b**. Since

$$\det[\mathbf{b}] = \chi_1, \chi_2, \chi_3, \ldots, \chi_{2N}, \tag{4.7}$$

at least one of χ_j must be zero where the flow is critical:

$$\chi_j = 0 \quad \text{for some } j. \tag{4.8}$$

In the case of the Fig. 5a, the magnitudes of some of the χ_j are finite but quite small upstream of the sill, rendering det[**b**] small. However, the magnitude of the eigenvalue (χ_6) that becomes zero at the sill remains relatively large upstream and downstream. As shown in Fig. 5b, its zero crossing is clearly defined.

A slightly more ambitious example of application of (4.4) or (4.8) involves a numerical simulation of an overflow in a parabolic channel (Fig. 6). Details of the numerical model and its use in studies of similar hydraulic flows in rectangular channels can be found in Helfrich et al. (1999) and Pratt et al. (2000). In short, the model solves the single-layer, shallow-water equations using a finite volume flux-limiting scheme that is designed to handle the complexities of rotating hydraulic flows (e.g., shocks, jumps, and layer outcropping). For the run in Fig. 6 the model is initialized in a uniform parabolic channel with $\alpha = 4$ and $h_0 = 0$ [see (4.6)] with a flow with uniform potential vorticity ($q = 1$) and

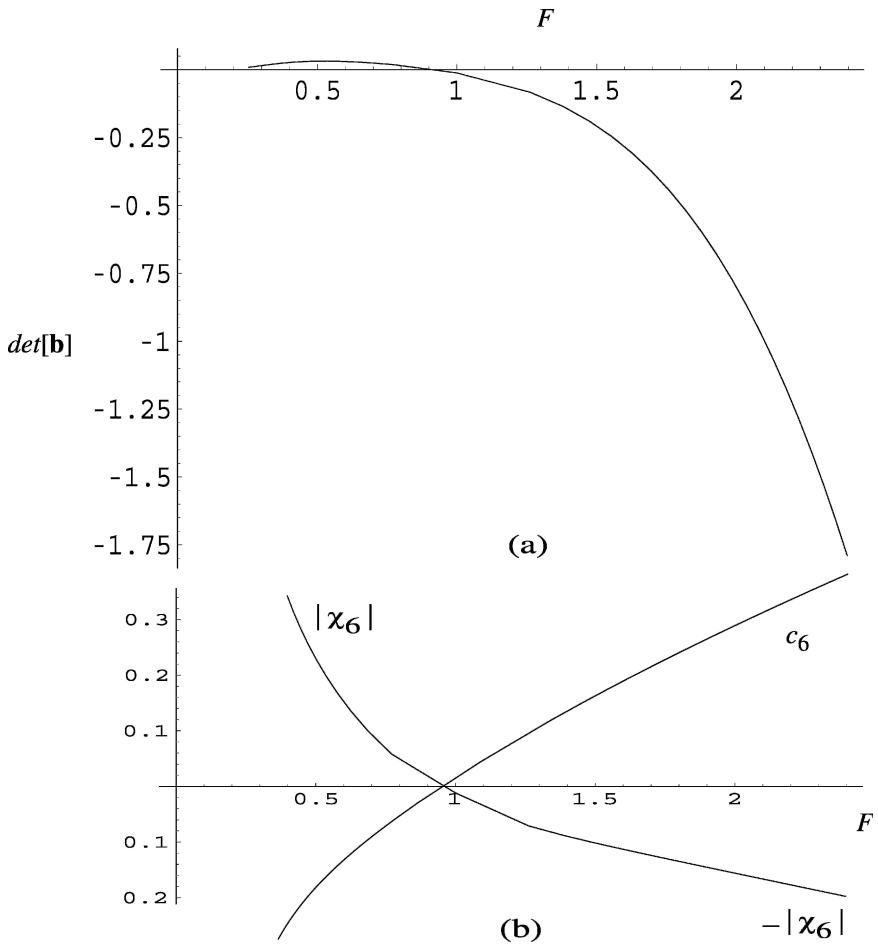

FIG. 5. (a) The value of det[**b**] as a function of Froude number for a flow with uniform potential vorticity in a parabolic channel and for the parameters specified in Fig. 4b. The magnitude of the eigenvalue χ_6 of **b** that has a zero crossing where det[**b**] does. For visual convenience $|\chi_6|$ is allowed to cross the Froude number axis where $|\chi_6|$ becomes zero. The wave speed c_6 of the corresponding wave mode (i.e., the mode whose speed is zero where $|\chi_6|$ is zero) is as calculated from (5.1).

semigeostrophic Froude number $F_p = 1.5$ [see (C.1)]. Between $t = 0$ and 2 a bump with amplitude $h_0 = 0.5$, centered at $y = 0$, is introduced into the flow. Figure 6a shows the free surface elevation at $t = 60$ after the introduction of the bump. Disturbances have propagated both upstream and downstream leaving a new hydraulically controlled flow in the vicinity of the bump. Figure 6b shows F_p calculated from (C.1) for the numerical solution at $t = 60$ assuming uniform $q = 1$. The jagged quality of F_p (and of the curves in Fig. 7) is a numerical artifact caused by the discrete representation of the edges of the flow on the numerical grid. While the numerically computed flow does not have uniform q in the wake of the upstream and downstream propagating disturbances, the Froude number based on uniform q indicates a hydraulic transition from sub to supercritical flow just downstream of the sill crest. The upstream/downstream asymmetry of the flow also indicates the presence of a hydraulic transition over the bump.

A direct determination of the critical section can be made by introducing a small disturbance at some section y in the Fig. 6a flow and integrating the model forward in time. Upstream and downstream propagation of the disturbance indicates locally subcritical flow while downstream-only propagation indicates supercritical flow. For this example, the critical section was found to lie between $0 \leq y \leq 1$, which is in good agreement with the uniform q prediction.

The value of det[**b**] based on $N = 3$ is calculated over a range of sections upstream and downstream of the sill (Fig. 7a). As before, this value crosses from positive to

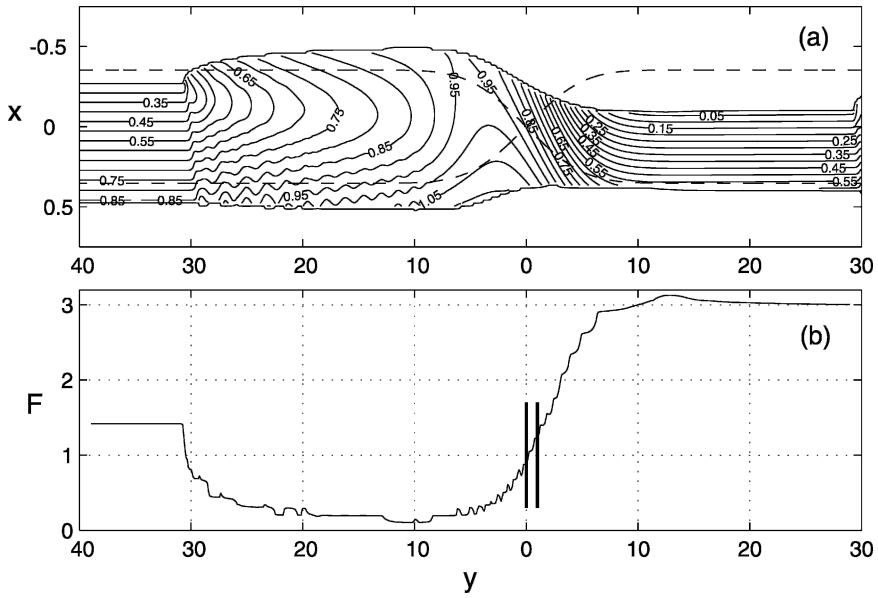

FIG. 6. Transient adjustment to a single-layer hydraulically controlled flow following the introduction of an obstacle in a parabolic channel. The initial flow has uniform potential vorticity $q = 1$ and $F_p = 1.5$ in a channel with $\alpha = 4$ and $h_0 = 0$ [see (4.6)]. A bump grows to a maximum height $h_0 = 0.5$ between $t = 0$ and $t = 2$. (a) Contours of the free surface elevation $h + d$ at $t = 60$. The solid bounding contours show the location of zero layer depth ($d < 0.001$). The dashed lines are the topographic contour $h = 0.5$. (b) The semigeostrophic Froude number F_p at $t = 60$, computed from (C.1) with $q = 1$. The critical section was determined independently to lie between the two vertical lines at $y = 0$ and $y = 1$ from the propagation of small localized disturbances introduced into the flow in (a).

negative values slightly downstream of the sill with relatively small magnitudes over the upstream range. On the other hand, the zero crossing of the associated eigenvalue (Fig. 7b) is less ambiguous. However, both calculations agree quite well with the estimates of the position of the critical section using F_p and by observation of wave propagation.

5. Direct calculation of the wave speed

The critical condition (4.4) will be most useful in analytical models, whereas (4.8) will be better suited to the evaluation of output from a numerical simulation. Application of (4.8) to the ocean, where data are typically collected at a moderate number of sections, is likely to be more problematic. The value of a particular eigenvalue χ_j at a section determines only whether the flow is critical or possibly not critical. The critical section (where one of the χ_j values crosses through zero) will almost certainly fall between two of the observed sections. One would therefore have to calculate the value of χ_j from one observed section to the next, making sure that the same eigenfunction (the same j) is followed. The bookkeeping is straightforward when the sections can be spaced closely enough so that χ_j varies gradually from one to the next, as in a numerical model. It is more difficult when the sections are widely spaced and the eigenfunctions undergo large changes. A procedure that is less elegant but better suited to observational data is direct calculation of the linear long-wave speeds c_j of the system. The result allows one to judge the flow at a particular section as subcritical or supercritical depending on whether the wave in question has positive or negative phase speed. Moreover, the eigenfunctions have a physical basis as wave modes that make them more identifiable from one section to the next. The following discussion assumes that the wave speed is real for the hydraulically relevant wave mode.

A method of calculation of c_j that is convenient and provides a direct connection with the Gill approach is based on a time-dependent version of the multiple streamtube model. Let the observed edge positions (Fig. 3b) and the corresponding interface elevations be given by $\boldsymbol{\gamma}_b = (\overline{x}_1, \overline{x}_2, \ldots, \overline{\eta}_1, \overline{\eta}_2, \ldots)^{\mathrm{T}}$. The positions x_i of the cell edges and the corresponding elevations η_i are now allowed to vary about these background positions and the resulting fluctuations $\boldsymbol{\gamma}' = (x_1', x_2', \ldots, \eta_1', \eta_2', \ldots)^{\mathrm{T}}$ are assumed to have $y - ct$ dependence. As

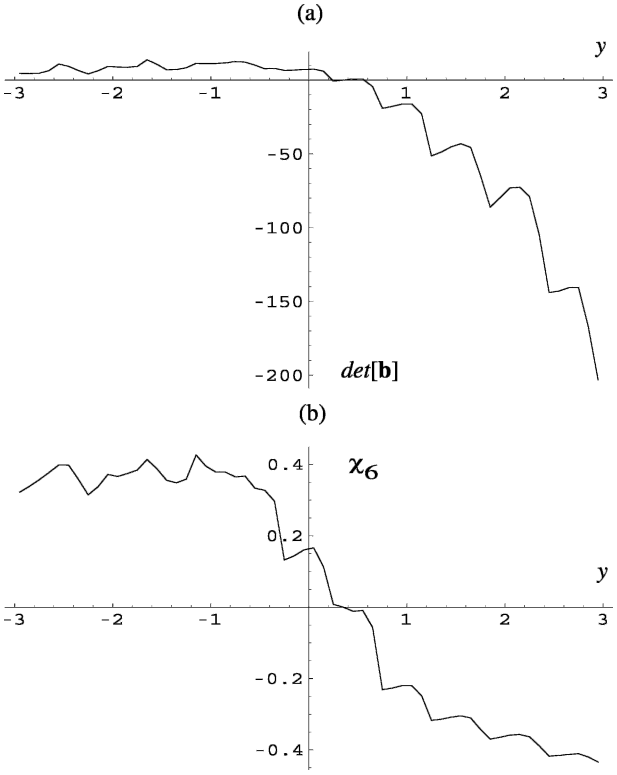

FIG. 7. Same as Fig. 5, but for the numerically generated flow shown in Fig. 6. The Froude number axis has been replaced by the y axis, with negative values indicating sections lying upstream of the sill.

shown in appendix D, $\boldsymbol{\gamma}_b'$ obeys the linear eigenvalue relation

$$[\mathbf{b}(\boldsymbol{\gamma}_b) - c\mathbf{a}(\boldsymbol{\gamma}_b)]\boldsymbol{\gamma}' = 0, \tag{5.1}$$

and thus the wave speeds c_j are the eigenvalues of the matrix $\mathbf{a}^{-1}(\boldsymbol{\gamma}_b)\mathbf{b}(\boldsymbol{\gamma}_b)$. Both $\mathbf{a}$ and $\mathbf{b}$ are defined in appendix D. The matrix $\mathbf{b}$ is identical to that defined in section 4, providing a link with the extended Gill formulation. Since

$$c_1c_2c_3 \times \cdots \times c_{2N} = \det[\mathbf{a}^{-1}\mathbf{b}] = \det[\mathbf{a}^{-1}]\det[\mathbf{b}],$$

the critical condition (4.4) implies that at least one of the speeds c_1, c_2, and so on, is zero.

The calculation of c_j based on the streamtube model should be equivalent to a calculation based on the discrete representation of the continuous equations for a linear normal mode. Our approach has a direct tie-in with Gill's approach. It also has built in variable cross-stream resolution, should one portion of the flow require higher resolution.

6. The significance of the local Froude number

The "local" Froude number is defined as

$$F = \frac{(u^2 + v^2)^{1/2}}{(g'd)^{1/2}}. \tag{6.1}$$

In traditional, one-dimensional ($u = 0$, $\partial/\partial x = 0$) models, hydraulic criticality corresponds to $F = 1$. The significance of F for hydraulic control in a flow with transverse variations ($\partial/\partial x \neq 0$) is less clear, but this has not prevented its appearance in discussions of models and data. For example, Rydberg (1980) based his theory of deep-water, rotating channel flow on the assumption that the $F = 1$ all across the critical section. In their report on a numerical simulation of the Strait of Gibraltar exchange flow, Izquierdo et al. (2001) present two-dimensional maps of the composite Froude number (the two-layer version of F) based on time-averaged fields. They show that this quantity falls above and below unity across certain sections; the Tarifa Narrows being one. They refer to such sections as "fragmentary" controls and write

> the term "control" is not appropriate to that situation because such a fragmentary control cannot provide efficient blocking (of) interfacial disturbances within a subcritical flow region and, hence, cannot completely determine the exchange rate in this region.

By "subcritical" they mean regions where the local composite Froude number falls below unity.

What is the significance of the local Froude number and how does it relate to stationary long-wave normal modes? Is it really true that a section in which F falls above and below unity provides only fragmentary and inefficient blocking? To resolve these issues, it is helpful to review a simple result from shallow water theory, as laid out by Courant and Friedrichs (1948) using the gas dynamics analogy. Consider a steady, shallow flow for which the value of F exceeds unity in a certain region (and in which the steady shallow water equations are therefore hyperbolic). If the velocity and depth at a particular point p within the region are given by $u = 0$, $v = v_0$, and $d = d_0$, then a localized disturbance generated at p will initially spread out in a widening circle as it is advected downstream (Fig. 8a). The radius of the circle will initially grow at rate $(gd_0)^{1/2}$ while the center of the circle will initially move forward at speed v_0. If $F = v_0/(g'd_0)^{1/2} > 1$ the disturbance will spread within a wedge of influence that spans the angle $2A$, where

$$A = \sin^{-1}(F_0^{-1}). \tag{6.2}$$

The "Froude" angle A and the edges of the wedge are analogous to the Mach angle and Mach lines of super-

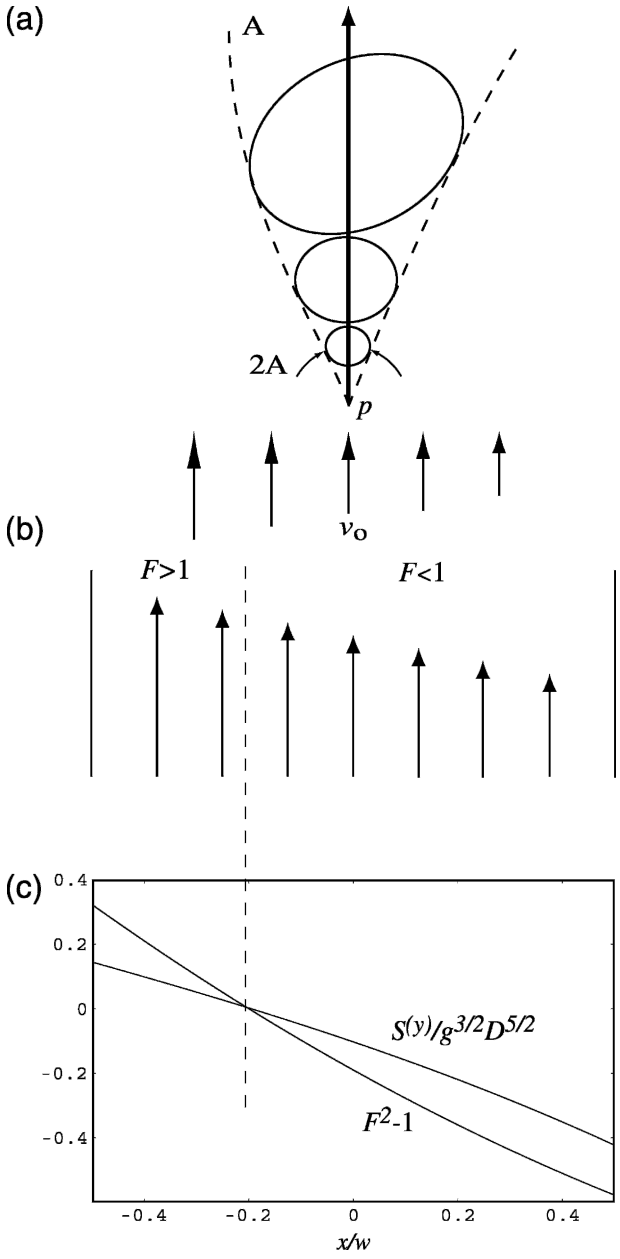

FIG. 8. (a) The wedge of influence downstream of a point p in a shallow flow with $F > 1$. The circles represent a spreading disturbance generated at p, and A is the Mach angle (or Froude angle) defined by the edges of the wedge. As the disturbance is advected downstream, it may become distorted by nonuniformities in the velocity or depth. (b) Plan view showing a hydraulically subcritical flow with constant shear s and depth d_0 [see (6.3)], with $sw = -0.5$, $\bar{v}/(gd_0)^{1/2} = 0.9$, and [from (6.4)], $c_-/(gd_0)^{1/2} = -0.13$. (c) The along-channel component $S^{(y)}$ of the local energy flux vector [(E.2)] for c_-. The value of $F^2 - 1$ is also shown and it shows that $S^{(y)}$ changes signs where F crosses unity.

sonic flow. The edges also define two of the three characteristic curves of the steady flow, the third being the steady streamlines. If the flow is nonuniform, as will generally be the case under rotation, the cone of influence still takes on the angle given by (6.2) near p but becomes distorted farther from p. The essential point is that localized disturbances propagate downstream. If $F < 1$, the disturbance circle spreads upstream and downstream (and the governing equations are no longer hyperbolic).

While the above description applies to a localized disturbance, hydraulics is generally concerned (for reasons already discussed) with long waves. These waves satisfy the sidewall boundary conditions and therefore have a cross-strait modal structure. Normal modes are important because the control results from a choking effect in which the entire flow is squeezed from below and from the sides. The wave that is instrumental in the control and blocking of the upstream flow must therefore sense the boundaries and satisfy the boundary conditions. It is easy to find examples where such waves can propagate upstream or remain stationary even where a portion of the flow across the section in question has $F > 1$. A simple example is the nonrotating flow with uniform depth and shear:

$$v = \bar{v} - sx, \quad u = 0, \quad d = d_0, \tag{6.3}$$

confined to a channel that spans $-w/2 < x < w/2$. A straightforward calculation show that this flow supports long, free surface gravity waves with speeds

$$c_\pm = \bar{v} \pm (gd_0 + s^2w^2/4)^{1/2}, \tag{6.4}$$

and thus the flow is hydraulically critical for $\bar{v} = (gd_0 + s^2w^2/4)^{1/2}$. It is also easy to find cases where the overall flow is hydraulically subcritical ($c_- < 0$ even though F exceeds unity across part of the channel cross section. An example of such a case (Figs. 8b, c) shows a band of flow with $F > 1$ on the left side of the channel (facing downstream) and $F < 1$ on the right.

The example of Fig. 8b may seem paradoxical. The long wave, which has a normal mode structure extending all across the channel, clearly propagates upstream even though localized disturbances must propagate downstream in the $F > 1$ band along the left wall. In addition, the wave is nondispersive and its energy must propagate upstream at the phase speed. The situation may be rendered less mysterious by noting that only the net (width integrated) disturbance energy is required to propagate upstream for the long wave. Positive energy flux in the $F > 1$ region can be offset by a larger negative energy flux in the $F < 1$ region. Figure 8c shows the

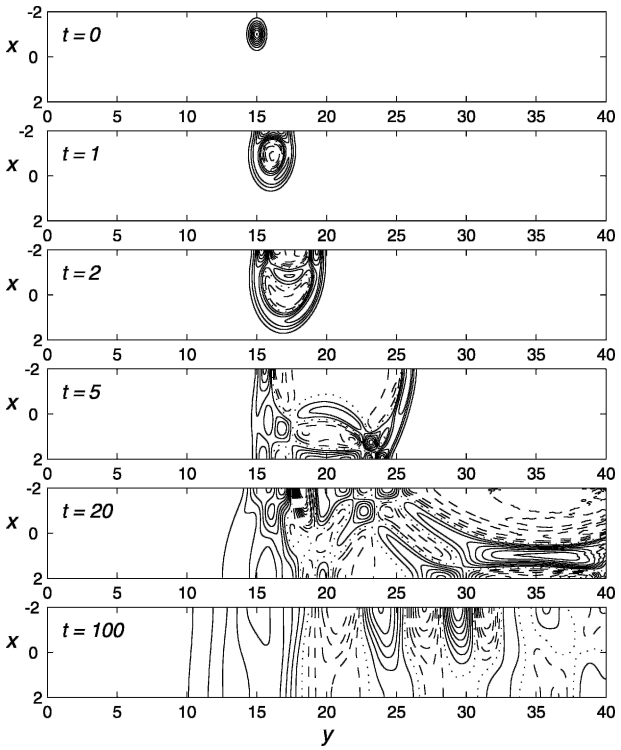

FIG. 9. (top to bottom) Evolution with time of a localized disturbance to a shallow, subcritical flow with constant vorticity. The background flow is of the form (6.3), with $sL/(gd_0)^{1/2} = 0.1$, $w/L = 4$, and $\bar{v}/(gd_0)^{1/2} = 1.0$, making $c_-/(gd_0)^{1/2} = -0.02$. Here L is the scale of the initial disturbance to the free surface elevation: $\eta/d_0 = 0.01 \exp\{-[2(x + L)L]^2 + [(y - 15L)/L]^2\}$. The contours are surface elevation with dashes indicating negative values. Times are nondimensionalized by $L/(gd_0)^{1/2}$.

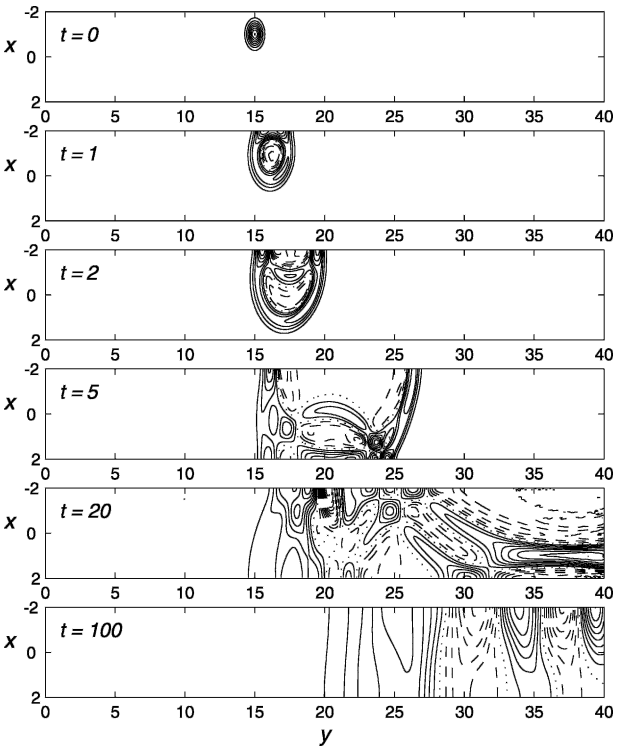

FIG. 10. Same as Fig. 9 except that $\bar{v}/(gd_0)^{1/2}$ has been increased to 1.1, making the initial flow supercritical, $c_-/(gd_0)^{1/2} = 0.08$.

local, along-channel, disturbance energy flux $S^{(y)} = gD\langle v'\eta\rangle + \frac{1}{2}V(D\langle v'^2\rangle + g\langle\eta^2\rangle)$ (appendix E) plotted across the channel; $S^{(y)}$ is positive where $F > 1$, as expected from our prior discussion. However, $S^{(y)}$ is negative over the whole right-hand portion of the channel, where $F < 1$.

Further insight into the role of localized disturbances, their ability to affect the upstream flow and their relationship to normal modes can be gained from two numerical simulations (Figs. 9 and 10). In the first example, we pose an initially steady flow of the form (6.3), with $\bar{v}$, s, and d_0 chosen to make $c_- < 0$ (subcritical flow) and such that $F > 1$ (< 1) to the left (right) of the channel centerline $x = 0$ (Fig. 9). At $t = 0$, a localized disturbance of small amplitude is introduced into the flow on the left side (facing downstream) of the channel, where $F > 1$. As predicted, the disturbance initially spreads in the downstream direction ($t = 1$ frame of Fig. 9). Eventually, some of the disturbance energy begins to leak into the right side of the channel, where $F < 1$ ($t = 2$) and some of this energy moves upstream ($t = 5$). By this time, the disturbance has become aware of both sidewalls and a normal mode structure is becoming evident in the upstream portion. The normal mode is characterized by phase lines roughly perpendicular to the channel axis and extending all across the channel. As the disturbance evolves, this structure becomes more evident ($t = 20$, 100). The background flow is subcritical with respect to the long-wave normal mode and this is reflected by propagation upstream of the original site of the disturbance. Upstream propagation is allowed all across the channel because disturbance energy can propagate upstream along the right wall and leak into the left side of the flow as it does so.

Figure 10 shows a similar example in which the initial flow is supercritical $c_- > 0$. Regions with $F > 1$ and $F < 1$ still exist on the left and right sides of the channel, but the $F > 1$ is expanded slightly from the previous case. The localized disturbance initially develops as before and a hint of upstream penetration of disturbance energy is observed along the right wall at $t = 20$. This is not surprising; after all it is this region where $F < 1$. However, as the normal mode structure emerges this trend is reversed and the entire disturbance moves downstream. Localized upstream propagation of information is possible within the $F < 1$ region, but only over

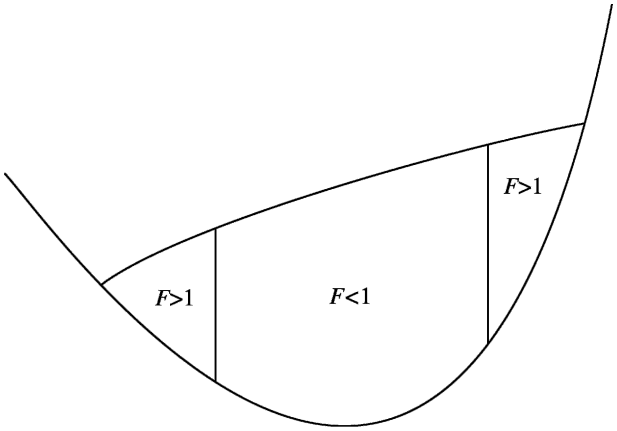

FIG. 11. The vanishing of the layer thickness coupled with finite velocity at the edges of the geostrophically balanced, inviscid flow means that the local Froude number F is infinite at the edges and that F will be > 1 along the edges (and perhaps over the whole cross section). In order for this flow to support a stationary wave, some region of $F < 1$ must exist to allow upstream local energy flux.

the time scale required for a normal mode to form. This scale is the time required for a free disturbance to traverse the channel width, reflecting off the channel walls several times, and therefore should equal 3 or 4 times $w/(gd_0)^{1/2}$. This scale equals 12–16 dimensionless time units of the simulation, about the time it takes for the normal mode structure to emerge. Thereafter upstream propagation is controlled by the speed c_- of the long normal mode, which in this case is >0.

These ideas also apply to a flow that is hydraulically critical. The implied nondispersive stationary wave must have zero group velocity and therefore zero net energy flux. If the fluid depth goes to zero at the edges (Fig. 11), and the velocity remains nonzero there, then F formally approaches ∞ at the edges. We would therefore expect to find bands of flow on either side of the channel in which $F > 1$. Since the characteristic curves of flow in these bands require downstream propagation of disturbance energy, there must exist a region with $F < 1$ in which upstream propagation of disturbance energy is permissible. The upstream flux of disturbance energy in this region must exactly cancel the downstream flux in the $F > 1$ regions, else the nondispersive wave cannot be stationary. These considerations suggest that for the situation shown in Fig. 11, *the local Froude number F must pass through unity at some interior point in order that the flow be hydraulically critical.* It also follows that *the flow must be hydraulically supercritical if $F \geq 1$ all across the section*, for then not even local upstream propagation is possible.

The remarks made in this section may not apply if the flow is unstable.

7. Discussion

We can now recommend procedures by which an investigator can establish a critical condition or assess the criticality of a given flow. If the flow is specified by an analytical model, (3.12) can be used to formulate a critical condition in terms of the dependent variables. Equation (3.16) then establishes a regularity (smoothness) condition that restricts the location of the critical section. If the model is question is numerical and the flow is subject to the usual hydraulic approximations (gradual variations along the channel and conservative) then (4.4) or its less noise-sensitive sibling (4.8) can be used to isolate the critical section(s). These formulas are based on a description in which the cross section of the flow is divided into N sections (streamtubes). The optimal value of N based on our numerical simulations and on the Faroe–Bank Channel flow (J. Girton 2005, personal communication) appears to lie in the range 3–5. Application requires that a $2N \times 2N$ matrix $\mathbf{b}$ [see (4.5)] be calculated at a series of closely spaced sections. All results to this point have been derived by generalizing Gill's method of treating hydraulically driven flows.

If the flow is observed and the observations have been made at a moderate number of sections, then there are two practical choices. A crude estimate of the criticality may be made by fitting the actual bottom topography to a parabola and calculating the parabolic Froude number F_p (Borenäs and Lundberg 1986; written out in our appendix C). The most problematic aspect of this approach is the estimation of the potential vorticity q of the flow (assumed constant in the theory), particularly if the observations are limited to hydrographic data. A more general approach is to calculate the phase speeds of the long, normal modes of the flow directly. We have laid out a procedure based on the streamtube description of the flow. The phase speeds are the eigenvalues of the matrix $\mathbf{a}^{-1}(\boldsymbol{\gamma}_b)\mathbf{b}(\boldsymbol{\gamma}_b)$ as defined in section 5. The type of wave is indicated by its cross-channel structure as reflected in the appropriate eigenfunction.

Of course, no observed flow is going to conform perfectly to usual hydraulic approximations. Perhaps the most serious departure for deep-ocean overflows is the presence of turbulence and dissipation. As suggested by the examples of appendix A, the extended Gill approach [as highlighted by (4.4)] continues to be valid in the presence of certain types of dissipation and forcing, provided that these effects enter the mathematical problem algebraically (and not as derivatives of the dependent variables). Turbulence and the closure problem present more formidable difficulties, but Stern

(2004) has recently suggested a variational criterion for a hydraulically controlled state in the underdetermined system.

We have also made some remarks concerning the significance of the local Froude number F in rotating hydraulics. In regions where $F > 1$, the characteristic curves of the steady flow indicate information propagation solely in the downstream direction. However, we have also noted that the presence of $F > 1$ across a portion of a section does not in itself prevent the upstream propagation (or the arrest) of long normal modes. We have also reconciled these two facts by noting that the local energy fluxes for the normal mode are directed downstream where $F > 1$, even though the net energy flux is upstream. We have further argued that at a critical section with realistic topography, where the layer thickness vanishes on the sides, and where the velocity remains finite on at least one side, that F must $=1$ somewhere across the section. This feature may well be more general, as suggested by Stern's (1974) criterion for control in a rectangular channel with positive v:

$$\int_{-w/2}^{w/2} \frac{1}{v^2 d}(1 - F^2)\, dx = 0.$$

Again, F must $= 1$ somewhere in $-w/2 < x < w/2$. The property can also be inferred from Stern's (2004) critical condition for flow over a sloping bottom. [The relationship following his (4.21) can be used to show that the right-wall Froude number is <1, whereas the Froude number on his left wall is infinite.]

Acknowledgments. This work was supported by National Science Foundation Grant OCE-0132903 and the Office of Naval Research under Grant N00014-01-1-0167. We are grateful to Ulrike Riemenschneider, Mary-Louise Timmermans, James Girton, and two anonymous reviewers for helpful comments.

APPENDIX A

Functionals with Nonlocal Dependence in y

The dependence of the flow on the local values of the geometric functions $h(y)$, $w(y)$, and so on, is a consequence of the assumptions of gradual variations in y and of the lack of forcing and dissipation. There are some flows that exhibit hydraulic behavior but are not subject to these restrictions. The governing functionals typically contain nonlocal dependence as expressed through integrals in y. Two examples, both in nondimensional form, are

$$G_P\left[d(y), \int_{y_0}^{y} f(d)\, dy'; h(y); q, y_0, \ldots \right] = \frac{q^2}{2d^2} + d + h + \alpha q^2 \int_{y_0}^{y} d^{-3}\, dy' = B(y_0) \quad \text{(A.1)}$$

and

$$G_{\mathrm{BL}}\left[d(y), \int_{y_0}^{y} \int_{y_0}^{y'} f(d)\, dy''\, dy'; h(y); F_0, y_0, \ldots \right] = \frac{F_0}{2d^2} + \frac{d}{F_0} + \frac{h}{F_0} + \frac{1}{F_0} \int_{y_0}^{y} \int_{y_0}^{y'} (d + 1)\, dy'\, dy = \frac{F_0}{2} - \frac{1}{F_0}. \quad \text{(A.2)}$$

Equation (A.1), which is derived by Pratt (1986), governs the flow of a shallow layer of depth $d(y)$ over an obstacle of height $h(y)$. Although conditions are assumed to vary gradually in y the direction, the fluid feels a bottom drag. Fixed parameters include the volume transport per unit width $q = vd$ and the drag parameter α. The presence of drag introduces an integration from an upstream location $y = y_0$ where the depth and velocity v are known, to the section under consideration. It can be shown independently that critical flow and hydraulic transitions occur under the usual condition ($v = d^{1/2}$) for an inviscid, single-layer, one-dimensional flow. Equation (A.2) governs the flow of a rotating, shallow layer over a uniform ridge on an infinite plane and can be derived from (5.8) of Baines and Leonard (1989). This flow is conservative but differs from traditional cases in that it varies rapidly in the direction (y) normal to the ridge. The variables d and h continue to represent depth and topographic height while F_0 represents the (fixed) Froude number of the flow far upstream of the ridge. It has been shown by Baines and Leonard that critical flow and hydraulic transitions again occur where $v = d^{1/2}$. In contrast to the usual result for gradually varying flows, the stationary waves in this case have zero wavelength (and are nondispersive in this limit).

The downstream integrations with respect to y in (A.1) and (A.2) imply that $d(y)$ depends on the upstream history of d and h and not just the local value of h, as assumed by Gill (1977). Nevertheless, we may derive the critical condition by following a train of thought similar to what has been used above. Suppose that the flow is subcritical or supercritical upstream and that it evolves in the downstream direction, passing through a critical section at $y = y_c$. By definition, a free stationary disturbance δd can exist at $y = y_c$ but not at any $y < y_c$. For the disturbance to be dynamically possible, it must not alter the value of the functional (G_P or G_{BL}) at $y = y_c$. For the case (A.1), it follows that

$$\lim_{\delta d \to 0} \left\{ \frac{G_P\left[d + \delta d, \int_{y_0}^{y_c} f(d + \delta d)\, dy'; h(y_c), q, y_0, \dots \right] - G_P\left[d, \int_{y_0}^{y_c} f(d)\, dy'; h(y_c), q, y_0, \dots \right]}{\delta d} \right\} = 0,$$

and evaluation of this limit leads to the correct condition $v = d^{1/2}$. A key feature is that the disturbance has zero amplitude in the interval $y_0 \le y < y_c$ and therefore has no effect on the value of the integral over that interval. Application of the same principle to (A.2) yields the same critical condition.

APPENDIX B

The Gill Approach Applied to a Continuous System of Conservation Laws

Each case discussed thus far has involved a finite number of degrees of freedom in the cross-stream direction. Such systems arise when the fluid can be partitioned into regions or layers having certain uniform properties such as density or potential vorticity. When these properties vary continuously, it is necessary to replace the index j by a continuously varying cross-stream coordinate z. This coordinate could be spatial or could represent a flow-based quantity such as density. It is assumed that the problem can be formulated in terms of a single variable, such as the streamfunction $\psi(y, z)$. The governing relationship may depend on the derivatives and integrals of ψ with respect to z, and thus (3.10) is replaced with

$$G\left\{ \psi(z, y), \frac{\partial \psi}{\partial z}, \frac{\partial^2 \psi}{\partial z^2}, \dots, \frac{\partial^M \psi}{\partial z^M}, \int f_1 \psi(\xi_1)\, d\xi_1, \int\int f_2[\psi(\xi_2)]\, d\xi_2\, d\xi_1, \dots; h(y), \dots; B(\psi), \dots \right\} = 0. \quad \text{(B.1)}$$

Boundary conditions applied at $z = z_1(y)$ and $z = z_2(y)$, say, add additional constraints of the form

$$F_i^{(j)} \left\{ \psi[z_i(y), y], \frac{\partial \psi}{\partial z_i}, \dots; h(y), \dots \right\} = C_i^{(j)} \qquad (i = 1, 2 \quad \text{and} \quad j = 1, N_b), \quad \text{(B.2)}$$

where N_b is the number of independent conditions at each boundary.

A hydraulically critical state $\psi_c(z)$ must support stationary disturbances and thus a perturbation $\varepsilon\tilde{\psi}(z)$ ($\varepsilon \ll 1$) must exist such that $\psi_c(z) + \varepsilon\tilde{\psi}(z)$ satisfies (B.1) and its boundary conditions (B.2) at a particular y:

$$G[\psi_c(z) + \varepsilon\tilde{\psi}(z), \dots; w(y), h(y), \dots] = C \quad \text{(B.3)}$$

and

$$F_i^{(j)}[\psi_c(z_i) + \varepsilon\tilde{\psi}(z_i), \dots; w(y), \dots] = C_i^{(j)}. \quad \text{(B.4)}$$

It follows that

$$(\delta G)_{w,h,\dots} = \left(\frac{\partial G}{\partial \psi} \right)_{\psi = \psi_c} \tilde{\psi}(z) = \lim_{\varepsilon \to 0} \frac{\{G[\psi_c(z) + \varepsilon\tilde{\psi}(z), \dots; w(y), \dots] - G[\psi_c, \dots; w(y), \dots]\}}{\varepsilon} = 0 \quad \text{(B.5)}$$

and similarly

$$[\delta F_i^{(j)}]_{w,h,\dots} = \left(\frac{\partial F_i^{(j)}}{\partial \psi} \right)_{\psi = \psi_c} \tilde{\psi}(z_i) = \lim_{\varepsilon \to 0} \frac{\{F_i^{(j)}[\psi_c(z_i) + \varepsilon\tilde{\psi}(z_i), \dots; w(y), \dots] - F_i^{(j)}[\psi_c(z_i), \dots; w(y), \dots]\}}{\varepsilon} = 0$$
$$(j = 1, 2), \quad (i = 1, 2, \dots, J). \quad \text{(B.6)}$$

Equation (B.5) is a linear, homogeneous integral-differential equation for $\tilde{\psi}(z)$, subject to the homogeneous, linear boundary conditions (B.6). Homogeneity follows from the fact that $\tilde{\psi} = 0$ is clearly a solution, and this property is related to the requirement that the disturbances are free [$w(y)$, etc., are held fixed]. In gen-

eral, the homogeneity of (B.8) and (B.6) implies that nontrivial solutions exist only for special values of the coefficients, which depend on $\psi_c(z)$. Any $\psi_c(z)$ that allows nontrivial solutions is a critical state and thus the critical condition is essentially a solvability condition. Examples are presented by Killworth (1992 and 1995).

If the derivatives and integrals in $(\delta G)_{w,h,\ldots} = [\delta G^{(j)}]_{w,h,\ldots} = 0$ are written using discrete approximations, then it should be possible to express the result in the form

$$L_{ij}(\psi_c)\tilde{\psi}_j = 0, \tag{B.7}$$

where $L_{ij}(\psi_c)$ is a coefficient matrix and $\tilde{\psi}_j$ is the discrete representation of $\tilde{\psi}(z)$. The solvability condition for (B.5) is

$$\det L_{ij} = 0, \tag{B.8}$$

and this is essentially the same as (3.12).

APPENDIX C

Parabolic Channel Solutions

In the present coordinate system, the layer depth and velocity profiles for flow with uniform potential vorticity q in a channel of parabolic cross section [see (6.5)] are given by

$$d(x,y) = \frac{1 + 2\alpha}{q \sinh(q^{1/2}w)}\{\sinh[q^{1/2}(x_1 - x)] - \sinh[q^{1/2}(x_4 - x)]\} + q^{-1}(1 + 2\alpha)$$

and

$$v(x,y) = \frac{1 + 2\alpha}{q^{1/2} \sinh(q^{1/2}w)}\{\cosh[q^{1/2}(x_4 - x)] - \cosh[q^{1/2}(x_1 - x)]\} + 2\alpha x,$$

where $x_1(y)$ and $x_4(y)$ are the positions of the left and right edges of the flow and $w = x_4 - x_1$ is the width of the flow. See Borenäs and Lundberg (1986) for more details.

The associated semigeostrophic Froude number, as originally written down by Borenäs and Lundberg (1986), is given by

$$F_p^2 = \frac{T^2(x_4 + x_1)^2}{(w - 2Tq^{-1/2})\{w - 2Tq^{-1/2} + (T^2 - 1)[w - (1 + 2\alpha)T\alpha^{-1}q^{-1/2}]\}}, \tag{C.1}$$

where $T = \tanh(q^{1/2}w/2)$. We have also derived the long-wave speeds of the system and found

$$c_{\pm} = \hat{v} \pm \langle \alpha^2 T^{-2}(w - 2Tq^{-1/2})\{w - 2Tq^{-1/2} + (T^2 - 1)[w - (1 + 2\alpha)T\alpha^{-1}q^{-1/2}]\}\rangle^{1/2}, \tag{C.2}$$

where $\tilde{v} = \alpha(x_4 + x_1)$. The Froude number (C.1) can also be deduced from this expression.

APPENDIX D

Long-Wave Speeds for Homogeneous Deep Overflow

The flow whose cross section is depicted in Fig. 3b is now allowed to vary with time to the extent that the positions of the cell walls and the (uniform in x) interfacial slope are functions of time. The velocity $v = v_n$ for each cell remains uniform in x but is discontinuous from one cell to the next. The velocity v_b of the overlying fluid is assumed to be zero. Consider the y-momentum equation for semigeostrophic flow, written in terms of variables evaluated along a material contour lying an infinitesimal distance to the right of the left edge $x = x_n(y, t)$ of cell n:

$$\frac{\partial}{\partial t}\{v[x_n(y,t),t] + x_n\} + \frac{\partial}{\partial y}\left\{\frac{v^2[x_n(y,t),t]}{2} + \eta[x_n(y,t),t]\right\} = 0, \tag{D.1}$$

where η has been scaled by a depth scale H, x and y by $(gH)^{1/2}/f$, t by f^{-1}, and v by $(gH)^{1/2}$.

The continuity equation for each cell is given by

$$\frac{\partial A_n}{\partial t} + \frac{\partial(\bar{v}_n A_n)}{\partial y}, \tag{D.2}$$

where A_n is the cell area, approximately $\frac{1}{2}(x_{n+1} - x_n)(\eta_{n+1} - h_{n+1} + \eta_n - h_n)$. If the latter is used along with the geostrophic relation $\bar{v}_n = (\eta_{n+1} - \eta_n)/(x_{n+1} - x_n)$, the continuity equation becomes approximated by

$$\frac{\partial}{\partial t}[(x_{n+1} - x_n)(\eta_{n+1} - h_{n+1} + \eta_n - h_n)] + \frac{\partial}{\partial y}[(\eta_{n+1} - \eta_n)(\eta_{n+1} - h_{n+1} + \eta_n - h_n)] = 0. \tag{D.3}$$

Boundary conditions are imposed by substituting $\eta_1 = h[x_1(y, t)]$ and $\eta_{N+1} = h[x_{N+1}(y, t)]$ into the $n = 1$ and $n = N$ versions of (D.1) and (D.3). When combined with the interior versions of the latter, one has $2N$ equations for the $N + 1$ values of x_n and the $N - 1$ values of η_n. After expansion of the differentiated terms, this system can be written in the form

$$\mathbf{a}\frac{\partial \boldsymbol{\gamma}}{\partial t} + \mathbf{b}\frac{\partial \boldsymbol{\gamma}}{\partial y} = 0, \tag{D.4}$$

where

$$\boldsymbol{\gamma} = (x_1, x_2, \ldots, x_N, x_{N+1}, \eta_2, \ldots, \eta_N)^{\mathrm{T}},$$

and

$$\mathbf{a} = \begin{pmatrix} a_{1,1} & a_{1,2} & 0 & 0 & \cdots & a_{1,N+2} & 0 & 0 & \cdots & 0 \\ 0 & a_{2,2} & a_{2,3} & 0 & \cdots & a_{2,N+2} & a_{2,N+3} & 0 & \cdots & 0 \\ 0 & 0 & a_{3,3} & a_{3,4} & \cdots & 0 & a_{3,N+3} & a_{3,N+4} & \cdots & 0 \\ \vdots & \vdots & \vdots & \vdots & \ddots & \vdots & \vdots & \vdots & \ddots & \vdots \\ 0 & 0 & 0 & a_{N,N} & a_{N,N+1} & 0 & 0 & 0 & \cdots & a_{N,2N} \\ a_{N+1,1} & a_{N+1,2} & 0 & 0 & \cdots & a_{N+1,N+2} & 0 & 0 & \cdots & \cdots \\ 0 & a_{N+2,2} & a_{N+2,3} & 0 & \cdots & a_{N+2,N+2} & a_{N+2,N+3} & 0 & \cdots & \cdots \\ 0 & 0 & a_{N+3,3} & a_{N+3,4} & \cdots & 0 & a_{N+3,N+3} & a_{N+3,N+4} & \cdots & \cdots \\ \vdots & \vdots & \vdots & \vdots & \ddots & \vdots & \vdots & \vdots & \ddots & \vdots \\ 0 & 0 & 0 & a_{2N,N} & a_{2N,N+1} & 0 & 0 & 0 & \cdots & a_{2N,2N} \end{pmatrix}$$

with $a_{n,n} = 1 + [2(\eta_{n+1} - \eta_n)/(x_{n+1} - x_n)^2]$, $a_{n,n+1} = 1 - [2(\eta_{n+1} - \eta_n)/(x_{n+1} - x_n)^2]$, $a_{n,N+n} = -[2/(x_{n+1} - x_n)]$, $a_{n,N+n+1} = [2/(x_{n+1} - x_n)]$, $a_{N+n,n} = -2[\eta_{n+1} - h(x_{n+1}) + \eta_n - h(x_n) + (x_{n+1} - x_n)(dh/dx_n)]$, $a_{N+n,n+1} = 2[\eta_{n+1} - h(x_{n+1}) + \eta_n - h(x_n) - (x_{n+1} - x_n)(dh/dx_{n+1})]$, $a_{N+n,N+n} = 2(x_{n+1} - x_n)$, and $a_{N+n,N+n+1} = 2(x_{n+1} - x_n)$, all for $n = 2, \ldots, N - 1$. In addition, $a_{1,1} = 1 + \{2[\eta_2 - h(x_1)]/(x_2 - x_1)^2\} - [2/(x_2 - x_1)]\ (dh/dx_1)$, $a_{1,2} = 1 - \{2[\eta_2 - h(x_1)]/(x_2 - x_1)^2\}$, $a_{1,N+2} = [2/(x_2 - x_1)]$, $a_{N,N} = 1 + \{2[h(x_{N+1}) - \eta_N]/(x_{N+1} - x_N)^2\}$, $a_{N,N+1} = 1 - \{2[h(x_{N+1}) - \eta_N]/(x_{N+1} - x_N)^2\} + [2/(x_{N+1} - x_N)]\ (dh/dx_{N+1})$, $a_{N,2N} = -[2/(x_{N+1} - x_N)]$, $a_{N+1,1} = -2[\eta_2 - h(x_2)]$, $a_{N+1,2} = 2[\eta_2 - h(x_2) - (x_2 - x_1)\ (dh/dx_2)]$, $a_{N+1,N+2} = 2(x_2 - x_1)$, $a_{2N,N} = -2[\eta_N - h(x_N) + (x_{N+1} - x_N)\ (dh/dx_N)]$, $a_{2N,N+1} = 2[\eta_N - h(x_N)]$, and $a_{2N,2N} = 2(x_{N+1} - x_N)$. Also, $a_{n,m} = 0$ for combinations of n and m other than those indicated.

The matrix $\mathbf{b}$ is just a nondimensional version of the $\mathbf{b}$ defined in section 6 and has a similarly sparse form: $b_{1,1} = \{2[\eta_2 - h(x_1)]^2/(x_2 - x_1)^3\} + \langle 1 - \{2[\eta_2 - h(x_1)]/(x_2 - x_1)^2\}\rangle(dh/dx_1)$, $b_{1,2} = -\{2[\eta_2 - h(x_1)]^2/(x_2 - x_1)^3\}$, $b_{1,N+2} = 1 + \{2[\eta_2 - h(x_1)]/(x_2 - x_1)^2\}$, $b_{N,N} = \{2[h(x_{N+1}) - \eta_N]^2/(x_{N+1} - x_N)^3\}$, $b_{N,N+1} = -\{2[h(x_{N+1}) - \eta_N]^2/(x_{N+1} - x_N)^3\} + \langle 1 + \{2[h(x_{N+1}) - \eta_N]/(x_{N+1} - x_N)^2\}\rangle(dh/dx_{N+1})$, $b_{N,2N} = 1 - \{2[h(x_{N+1}) - \eta_N]/(x_{N+1} - x_N)^2\}$, $b_{N+1,1} = -2[\eta_2 - h(x_2)](dh/dx_1)$, $b_{N+1,2} = -2[\eta_2 - h(x_1)](dh/dx_2)$, $b_{N+1,N+2} = 2[2\eta_2 - h(x_2) - h(x_1)]$, $b_{2N,N} = 2[\eta_N - h(x_{N+1})](dh/dx_N)$, $b_{2N,N+1} = 2[\eta_N - h(x_N)](dh/dx_{N+1})$, and $b_{2N,2N} = -2[2\eta_N - h(x_{N+1}) - h(x_N)]$. In addition, $b_{n,n} = [2(\eta_{n+1} - \eta_n)^2/(x_{n+1} - x_n)^3]$, $b_{n,n+1} = -[2(\eta_{n+1} - \eta_n)^2/(x_{n+1} - x_n)^3]$, $b_{n,N+n} = 1 - [2(\eta_{n+1} - \eta_n)/(x_{n+1} - x_n)^2]$, $b_{n,N+n+1} = 1 + [2(\eta_{n+1} - \eta_n)/(x_{n+1} - x_n)^2]$, $b_{N+n,n} = -2(\eta_{n+1} - \eta_n)(dh/dx_n)$, $b_{N+n,n+1} = -2(\eta_{n+1} - \eta_n)(dh/dx_{n+1})$, $b_{N+n,N+n} = -2[2\eta_n - h(x_n) - h(x_{n+1})]$, and $b_{N+n,N+n+1} = 2[2\eta_{n+1} - h(x_n) - h(x_{n+1})]$, all for $n = 2, 3, \ldots, N - 1$. Also $a_{n,m} = 0$ for combinations of n and m other than those indicated.

If the flow consists of small-amplitude disturbances $\boldsymbol{\gamma}'(y - ct)$ propagating on a background state $\overline{\boldsymbol{\gamma}}$, then linearization of (B.3) about this state leads to

$$[\mathbf{b}(\boldsymbol{\gamma}_b) - c\mathbf{a}(\boldsymbol{\gamma}_b)]\boldsymbol{\gamma}' = 0.$$

The possible wave speeds c are the eigenvalues of $\mathbf{a}^{-1}(\boldsymbol{\gamma}_b)\mathbf{b}(\boldsymbol{\gamma}_b)$. The dimensional wave speeds are given by $(gH)^{1/2}c$. The eigenvector $\boldsymbol{\gamma}_0$ contains the departures of $x_1, x_2, \ldots, \eta_1, \eta_2, \ldots$ from the basic state, and it must be kept in mind that the each interface elevation departure, η_n', is the difference between the elevation on the moving edge $x = x_n$ and the fixed basic-state elevation at the nearby mean value of x_n.

APPENDIX E

Energy Flux Vector

Consider the energy flux for a disturbance propagating on a general background flow $v = V(y)$, $u = 0$, and $d = D(y)$ in a rotating channel of variable bottom el-

evation $h(y)$. Small amplitude disturbances v', u', and η with a long-wave character ($v' \gg u'$ and $\partial/\partial x \gg \partial/\partial y$) obey the linear shallow-water equations for long waves:

$$fv' = g\frac{\partial \eta}{\partial x}, \qquad \text{(E.1a)}$$

$$\frac{\partial v'}{\partial t} + V\frac{\partial v'}{\partial y} + u'\frac{\partial V}{\partial x} + fu' = -g\frac{\partial \eta}{\partial y}, \qquad \text{(E.1b)}$$

and

$$\frac{\partial \eta}{\partial t} + V\frac{\partial \eta}{\partial y} + u'\frac{\partial D}{\partial x} + D\left(\frac{\partial u'}{\partial x} + \frac{\partial v'}{\partial y}\right) = 0. \qquad \text{(E.1c)}$$

Multiplication by Du', Dv', and gD, respectively, and summation of the products leads to the long-wave energy equation:

$$\frac{\partial}{\partial t}\left(\frac{Dv'^2 + g\eta^2}{2}\right) = -\nabla \cdot \left\{\left[gDv'\eta + \frac{1}{2}V(Dv'^2 + g\eta^2)\right]\mathbf{j} + gDu'\eta\mathbf{i}\right\} - u'v'D\frac{dV}{dy} - gu'\eta\frac{dD}{dy}.$$

For a disturbance proportional to $e^{il(y-c-t)}$ and with c real, it can easily be shown from (E.1a) that v' and η are in phase in the y direction, whereas (E.1b) implies that u' is out of phase with either. Therefore the cross-channel energy flux $gDu'\eta$ and the kinetic and potential energy conversion terms $[u'v'D(dV/dy)$ and $g'u'\eta(dD/dy)]$ will vanish after integration with respect to y over a wavelength. The local, along-channel energy flux is therefore

$$S^{(y)} = gD\langle v'\eta\rangle + \frac{1}{2}V(D\langle v'^2\rangle + g\langle\eta^2\rangle), \qquad \text{(E.2)}$$

where $\langle\,\rangle$ indicates an average with respect to y over a wavelength.

REFERENCES

Armi, L., 1986: The hydraulics of two flowing layers of different densities. *J. Fluid Mech.,* **163,** 27–58.

Baines, P. G., 1995: *Topographic Effects in Stratified Flows*. Cambridge University Press, 482 pp.

——, and B. P. Leonard, 1989: The effects of rotation on flow or a single layer over a ridge. *Quart. J. Roy. Meteor. Soc.,* **115,** 293–308.

Borenäs, K. M., and P. A. Lundberg, 1986: Rotating hydraulics of flow in a parabolic channel. *J. Fluid Mech.,* **167,** 309–326.

——, and A. Nikolopoulos, 2000: Theoretical calculations based on real topography of the deep-water flow through the Jungfern Passage. *J. Mar. Res.,* **58,** 709–719.

Courant, R., and K. O. Friedrichs, 1976: *Supersonic Flow and Shock Waves.* Interscience, 464 pp.

Dalziel, S. B., 1991: Two-layer hydraulics: A functional approach. *J. Fluid Mech.,* **223,** 135–163.

Engqvist, A., 1996: Self-similar multi-layered exchange flow through a contraction. *J. Fluid Mech.,* **328,** 49–66.

Gerdes, F., C. Garrett, and D. Farmer, 2002: On internal hydraulics with entrainment. *J. Phys. Oceanogr.,* **32,** 1106–1111.

Gill, A. E., 1977: The hydraulics of rotating-channel flow. *J. Fluid Mech.,* **80,** 641–671.

Hansen, B., W. R. Turrell, and S. Osterhus, 2001: Decreasing overflow from the Nordic seas into the Atlantic Ocean through the Faroe Bank Channel since 1950. *Nature,* **411,** 927–930.

Helfrich, K. R., A. Kuo, and L. J. Pratt, 1999: Nonlinear Rossby adjustment in a channel. *J. Fluid Mech.,* **390,** 187–222.

Hugoniot, P. H., 1886: Sur un théorème relatif au mouvement permanent et à l'écoulement des fluids. *C. Roy. Acad. Sci. Paris,* **103,** 1178–1181.

Izquierdo, A., L. Tejedor, D. V. Sein, J. O. Backhaus, P. Brandt, A. Rubino, and B. A. Kagan, 2001: Control variability and internal bore evolution in the Strait of Gibralter: A 2-D two-layer model study. *Estuarine Coastal Shelf Sci.,* **53,** 637–651.

Killworth, P. D., 1992: On hydraulic control in a stratified fluid. *J. Fluid Mech.,* **237,** 605–626.

——, 1995: Hydraulic control and maximal flow in rotating stratified hydraulics. *Deep-Sea Res.,* **42,** 859–871.

Long, R. R., 1954: Some aspects of the flow of stratified fluids. Part II: Experiments with a two-fluid system. *Tellus,* **6,** 97–115.

Pratt, L. J., 1986: Hydraulic control of sill flow with bottom friction. *J. Phys. Oceanogr.,* **16,** 1970–1980.

——, and L. Armi, 1987: Hydraulic control of flows with nonuniform potential vorticity. *J. Phys. Oceanogr.,* **17,** 2016–2029.

——, K. R. Helfrich, and E. Chassignet, 2000: Hydraulic adjustment to an obstacle in a rotating channel. *J. Fluid Mech.,* **404,** 117–149.

Reynolds, O., 1886: On the flow of gases. *Philos. Mag.,* **21** (5), 185–198.

Rydberg, L., 1980: Rotating hydraulics in deep-water channel flow. *Tellus,* **32,** 77–89.

Smeed, D. A., 2000: Hydraulic control of three-layer exchange flows: Application to the Bab al Mandab. *J. Phys. Oceanogr.,* **30,** 2574–2588.

Stern, M. E., 1974: Comment on rotating hydraulics. *Geophys. Fluid Dyn.,* **6,** 127–130.

——, 1980: Geostrophic fronts, bores, breaking and blocking waves. *J. Fluid Mech.,* **99,** 687–703.

——, 2004: Local "mean field" theory of hydraulically controlled strait flow. *J. Phys. Oceanogr.,* **34,** 1692–1701.

Whitehead, J. C., 1989: Internal hydraulic control in rotating fluids—Applications to oceans. *Geophys. Fluid Dyn.,* **48,** 169–192.

——, A. Leetma, and R. A. Knox, 1974: Rotating hydraulics of strait and sill flows. *Geophys. Fluid Dyn.,* **6,** 101–125.